

Repairing Effect of Fibronectin and Its Compositions on Damaged Skin

Li Kui¹; Liu Jia-wei¹; Lin Guang-xin¹; Li Yue-yan¹; Li Mei²; Zhang Fan²; Chen Yu-ying²;
Shi Hui-zhe¹; Wan Yang¹; Xia Li-ming¹

¹Guangzhou Jnumeso Bio-technology Co.,Ltd, GuangZhou, GuangDong

²Guangzhou Yiyang Biotechnology Co.,Ltd, GuangZhou, GuangDong

Abstract

Sensitive skin (SS) and damaged skin (DS) are both in a state of high reactivity. They are prone to subjective symptoms such as burning, stinging, itching, and tightness, with or without objective signs like erythema, scaling, and telangiectasia, which significantly impact the quality of life of affected individuals. Therefore, we attempt to creating a novel component combination by integrating Fibronectin(FN) with Soluble Proteoglycan(SP) and Artemia Extract(ART) together, leveraging their synergistic effects to enhance FN's functional efficacy. Initially, the bioactivity of the FN-based complex was validated in vitro. Results demonstrated that the complex significantly enhanced cellular viability, accelerated wound closure in scratch assays, upregulated key genes associated with stratum corneum barrier function, and suppressed UVB-induced IL-6 secretion in a radiation-damage model. Furthermore, in a randomized, double-blind, placebo-controlled clinical trial, the FN-based complex demonstrated significant efficacy in reducing erythema (decreased a* value) and restoring skin barrier function (reduced transepidermal water loss, TEWL) following microneedle arrays and tape-stripping-induced damage, with no reported adverse events. Collectively, these findings highlight the therapeutic potential of the FN-based complex as a novel dermatological intervention for managing both SS and DS.

Keywords: Sensitive skin; Damaged skin; Fibronectin; Soothing; Repairing

1.Introduce

Normal skin is susceptible to developing Sensitive Skin (SS) or Damaged Skin (DS) when exposed to various stressors including environmental aggressors, chemical irritants, physical friction, or minimally invasive aesthetic procedures. Both SS and DS represent hyperreactive cutaneous states characterized by neurosensory symptoms (burning, stinging, itching and tightness) that may present with or without clinical manifestations such as erythema, scales and capillary dilatation, significantly impairing quality of life of affected individuals. It is currently thought that the pathogenesis involves three key pathways: skin barrier dysfunction, neurovascular inflammation, and immune system dysregulation [1].

The compromised skin barrier plays a pivotal role in SS/DS development. Structural damage to the stratum corneum and disrupted intercellular lipid matrix lead to elevated transepidermal water loss and nutrient depletion[2]. This barrier impairment

results in stratum corneum thinning and increased epidermal permeability, facilitating enhanced penetration of exogenous substances^[3]. Such barrier defects heighten susceptibility to stressors, triggering inflammatory cascades that manifest clinically as dryness and redness-hallmark features of SS/DS. Additionally, hyperactive cutaneous sensory neurons mediate characteristic neurosensory symptoms through upregulated TRP channel signaling^[4-5]. Therefore, effective intervention requires a tripartite approach targeting barrier restoration, inflammation control, and neurosensory modulation.

Fibronectin (FN), a 450kD dimeric glycoprotein composed of two 220kD subunits linked by disulfide bonds^[6], demonstrates therapeutic potential for skin repair. Its established biological functions - including stimulation of cellular proliferation, migration, and tissue regeneration^[7] - mirror the key stages of wound healing (hemostasis, inflammation, proliferation, remodeling)^[8]. As illustrated in Fig 1, FN's mechanism particularly suits minimally invasive skin repair by promoting keratinocyte viability, enhancing tight junction formation, and suppressing inflammatory mediators - all critical for SS/DS management.

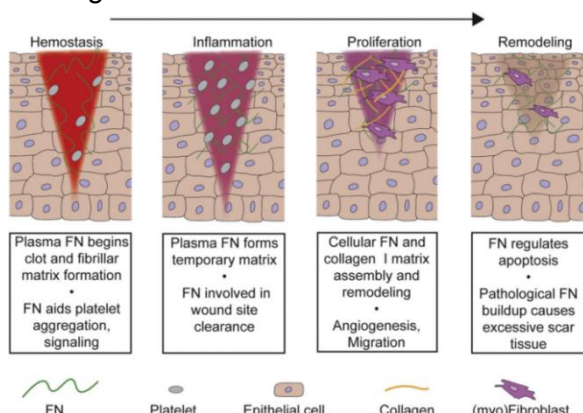


Fig1. An overview of FN signaling during the stages of wound healing

This study developed a novel bioactive complex combining FN with Artemia extract (ART) and soluble proteoglycans (SP). ART, derived from marine plankton, contains diguanosine tetraphosphate which upregulates HSP70 expression and enhances FN phosphorylation to facilitate extracellular matrix deposition^[9-10]. SP, glycosaminoglycan-protein conjugates, possess EGF-binding domains that potentiate FN's effects by accelerating epidermal turnover through EGFR activation^[11].

We first validated the complex's efficacy through comprehensive in vitro assays. Subsequent in vivo evaluation employed standardized skin perturbation models (microneedle arrays and tape stripping) on human volunteers to assess clinical reparative capacity.

2.Materials

Fibronectin (FN) : Solution, effective content 500ppm;
 Soluble Proteoglycan (SP) : Powder, 100% effective content;
 Artemia extract(ART) : Solution, effective content 0.5%;
 FN's complex: Mix FN, ART and SP in a certain proportion.

3.Methods

3.1 In Vitro Testing

3.1.1 Cell culture:

HaCaT keratinocytes (Chinese Academy of Sciences, Kunming, China) were cultured in Dulbecco's modified Eagle's medium (DMEM, Gibco, USA) supplemented with 10% fetal bovine serum and 1% penicillin/streptomycin (Gibco). Human skin fibroblasts (HSF) were purchased from Beijing EallBio Biomedical Technology, which were cultured in Dulbecco's Modified Eagle Medium/Nutrient Mixture F-12 (DMEM/F12, Gibco, USA), also supplemented with 10% fetal bovine serum and 1% penicillin/streptomycin (Gibco) as HaCaT cells. Both HaCaT keratinocytes and HSF cells were incubated at 37 °C in a humidified atmosphere containing 5% CO₂.

3.1.2 UVB radiation:

HaCaT cells were divided into three groups: the control group, the model group, ie UV radiated group, and the test sample group. The control group received no treatment. Prior to UVB irradiation, the culture medium was completely removed from the culture dishes. To ensure uniform irradiation and eliminate potential interference from medium components, the cells were gently rinsed twice with phosphate-buffered saline (PBS) to remove any residual medium and metabolic byproducts. Then 300 mJ/cm² doses of UVB was used to irradiate HaCaT keratinocytes, during irradiation, a thin layer of PBS was maintained on the cell surface to prevent dehydration, as PBS exhibits minimal UVB absorption.

3.1.3 Cell viability assay:

HaCaT keratinocytes were seeded in 96-well plates and treated with test sample for 48 h. The effect of different test sample concentrations on keratinocyte viability was assessed using the CCK-8 assay to evaluate the ability of cell proliferation. Cell viability (%) was calculated by measuring absorbance at 450 nm using a microplate reader (TECAN, Mannedorf, Switzerland).

3.1.4 Quantitative Real-Time PCR (qRT-PCR):

Total RNA was extracted using HiPure Total RNA Mini Kit (Magen, Guangzhou, China) following the protocol, which was then reverse transcribed to cDNA, then qRT-PCR was performed to assess gene expression level. Target gene PCR reactions were quantitated using Takara's RR820A TB Green Premix Ex Taq II (Tli RNaseH Plus). PCR reaction system (20 μL): TB Green Premix 10 μL, cDNA template 2 μL, forward and reverse primers 0.4 μL each, double distilled water 7.2 μL. PCR reaction conditions: 96 °C 1 min, 95 °C 15s, 60 °C 1 min, 95 °C 15s, total 40 cycles. Using the internal reference gene GADPH, the 2-ΔΔC_t technique was used to determine the target gene's relative expression.

3.1.5 Cell mobility assay:

Confluent HSF cells were wounded with a micropipette tip and immediately placed in 1% serum-containing medium supplemented with test sample. Bright-field images of wounded monolayers were obtained immediately after wounding (0 h) and at 24h thereafter as indicated. The extent of wound closure was quantified by obtaining three wound measurements for each of three random fields (× 100) per wound, and all wound conditions were performed in triplicate.

3.2 In Vivo Testing

3.2.1 Model establishment

Standardized skin barrier disruption was achieved through two complementary methods: (1) 40 consecutive D-squame tape stripping procedures to sequentially remove stratum corneum layers; (2) application of sterile mesotherapy microneedle arrays (0.15 mm length) with 30-second dwell time to simulate minimally invasive aesthetic damage.

3.2.2 Testing process

We performed a randomized, double-blind, placebo-controlled clinical study involving six healthy adult volunteers (5 females, 1 male; age range 26-58 years) to evaluate the reparative and anti-irritant efficacy of the FN-based complex. The study employed a split-body design with two treatment arms: (1) placebo control (sterile distilled water) and (2) active treatment (25% FN-based complex). Test materials were randomly allocated to designated forearm sites following standardized randomization protocols.

3.2.3 Test data

Erythema intensity (a* value) measured using the Delfin DCC1201, including 15-minute and 30-minute exposure periods for therapeutic assessment.

Skin barrier function evaluated via transepidermal water loss (TEWL) measurements using the Delfin SWL5001, including D1 and D7 exposure periods for therapeutic assessment.

3.3 Statistical Analysis

All the results expressed as mean \pm standard deviation (SD) were statistically analyzed using Student's *t*-test and one-way ANOVA using IBM SPSS Statistics 26 software. The significance levels were indicated as follows: * $P < 0.05$, ** $P < 0.01$, and *** $P < 0.001$.

4.Result & Discussion

4.1 In vitro Testing:

4.1.1 Cell viability test

Dose-response analysis revealed that the FN-based complex significantly enhanced HaCaT keratinocyte proliferation in a concentration-dependent manner, demonstrating its capacity to stimulate epidermal cell renewal. Quantitative assessment showed that treatment with 10% FN complex increased cellular proliferation by 18.28% ($p < 0.001$) compared to untreated controls (Fig 2).

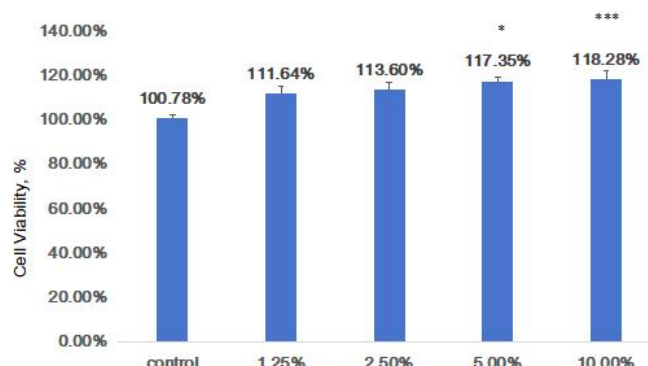


Figure2.FN-base complex effect on cell viability. vs control

4.1.2 Upregulated key genes associated with skin barrier function

The FN-based complex demonstrated concentration-dependent upregulation of key epidermal barrier genes in HaCaT keratinocytes, significantly enhancing expression of tight junction protein ZO-1 (18% increase, p<0.05) and differentiation marker involucrin (IVL) (45% increase, p<0.001) at 10% concentration (Fig 3). These findings substantiate the complex's barrier-restorative potential through dual modulation of cell-cell junctions and terminal differentiation processes.

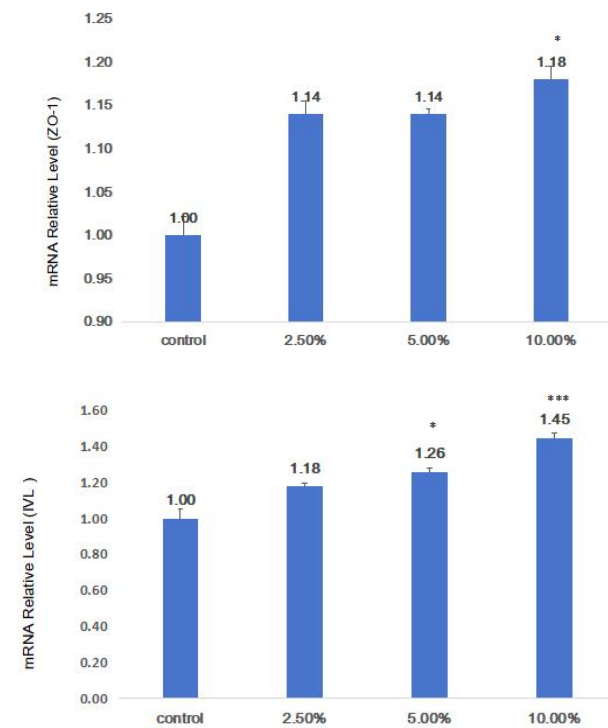


Figure3. FN-base complex effect on mRNA Relative Level ZO-1 and IVL.vs control

4.1.3 Cell migration test

The FN-based complex exhibited a concentration-dependent enhancement of human skin fibroblast (HSF) migration capacity, demonstrating its wound repair potential. Quantitative analysis revealed significant increases in migratory activity of 56.54% (1.5% concentration, p<0.001) and 60.64% (2.5% concentration, p<0.001) compared to untreated controls (Fig 4), Fig 5 showed wound closure in scratch assays, suggesting dose-responsive therapeutic effects on cutaneous wound healing.

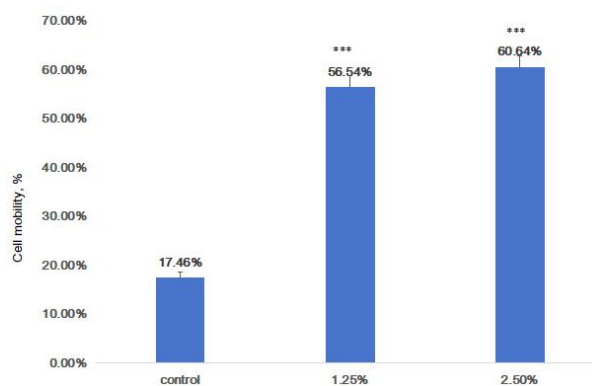


Figure4. FN-base complex effect on cell migration.vs control

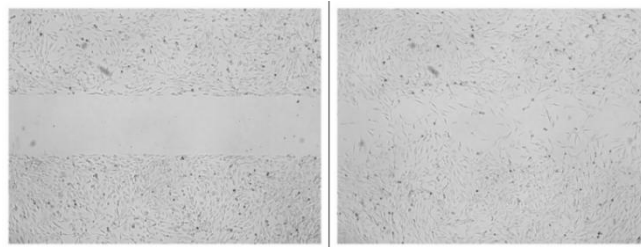


Figure5. FN-base complex(2.5%) effect on cell migration

4.1.4 Inhibition of inflammatory factors

The FN-based complex demonstrated significant concentration-dependent inhibition of UVB-induced IL-6 secretion in HaCaT keratinocytes. Quantitative q-PCR analysis revealed 35.3% (2.5% concentration, * $p^*<0.001$) and 48.3% (10% concentration, * $p^*<0.001$) suppression of this pro-inflammatory cytokine compared to UVB-irradiated controls (Fig 6), indicating potent anti-inflammatory activity through modulation of photodamage responses.

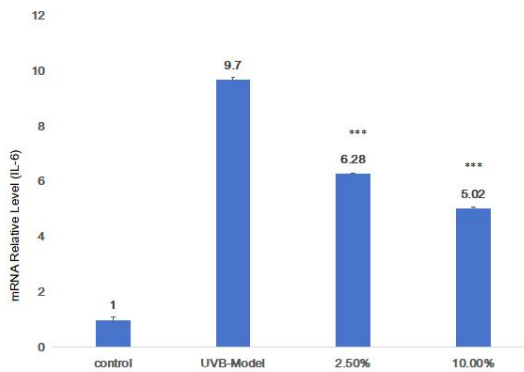


Figure6. FN-base complex effect on inhibition of IL-6 in UVB-Model. vs UVB-Model

4.2 In vivo testing:

4.2.1 In vivo testing of microneedle arrays modeling

As demonstrated in Figure 7, TEWL significantly increased following microneedle array application, confirming successful barrier disruption (model validation). Both the placebo and 25% FN-based complex sample groups exhibited rapid recovery of erythema (a^* value reduction) post-application. Notably, the FN-treated group showed statistically significant differences in a^* value reduction compared to both baseline ($p<0.05$) and placebo controls ($p<0.05$) within 30 minutes, demonstrating immediate anti-inflammatory and erythema-reducing efficacy.

While TEWL values in both groups returned to baseline (D0) levels by D1, the FN-treated group displayed further barrier enhancement by D7, with significantly lower TEWL versus placebo ($p<0.05$). These findings collectively indicate that the FN-based complex not only provides rapid symptomatic relief but also promotes sustained barrier restoration following microneedle arrays induced damage.

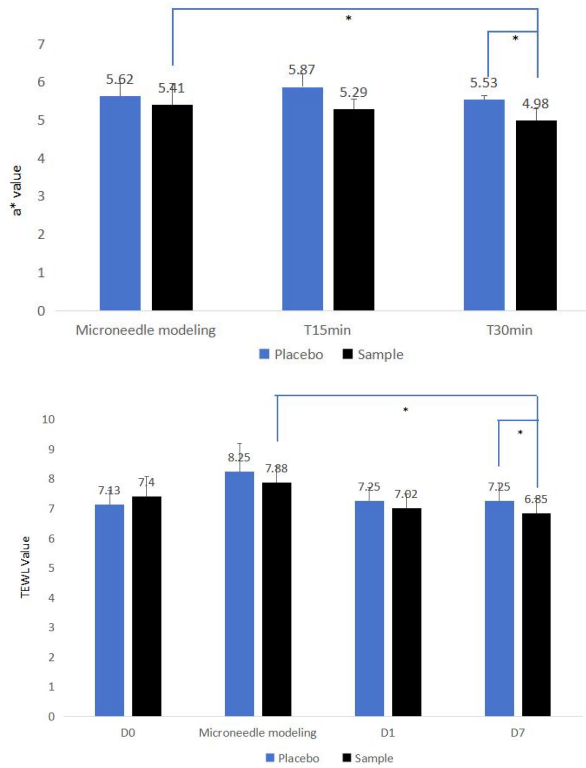
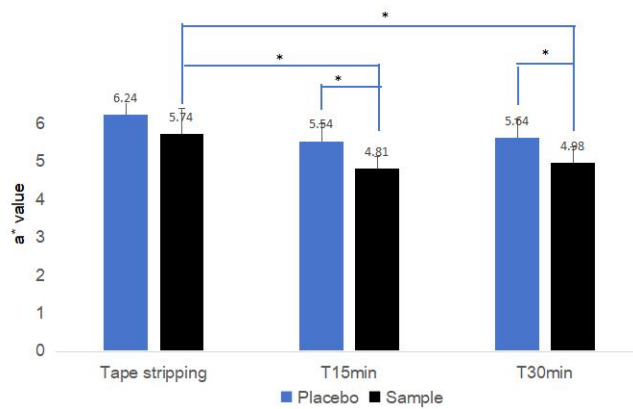


Figure 7. Analysis of a^* and TEWL value in Placebo and sample treated area

4.2.2 In vivo testing of tape stripping modeling

As illustrated in Figure 8, TEWL significantly increased following tape stripping, confirming successful barrier disruption (model validation). The 25% FN-based complex sample groups facilitated erythema reduction compared to baseline and placebo ($p<0.05$) within 15 and 30 minutes. Notably D7, the sample exhibited: (1) 26.6% lower TEWL versus post-modeling values ($p<0.001$) ; (2) 8.7% improvement compared to placebo ($p<0.001$).

These results demonstrate that the FN-based complex provides immediate anti-inflammatory/erythema-reducing effects and sustained barrier restoration exceeding placebo efficacy.



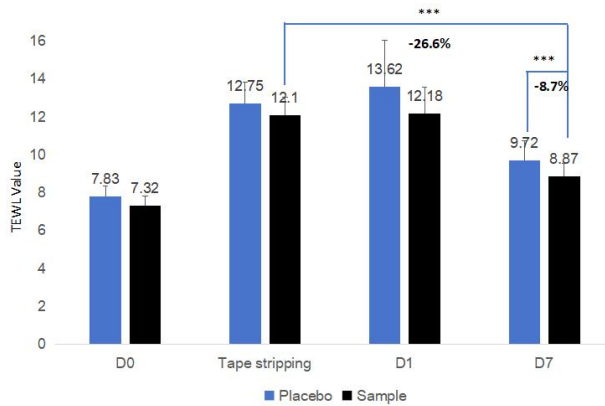


Figure8. Analysis of a* and TEWL value in Placebo and Sample treated area

Through microneedle arrays or tape tripping modeling, the FN-base complex demonstrated the effects of soothing redness and repairing, but the skin recovery processes under the two modeling methods were slightly different. It can be proved that the damage to the skin barrier caused by tape tripping is more severe, we found that the skin TEWL basically returned to the initial level on D1 in the microneedle arrays modeling, while not return to the initial level on D7 in the tape tripping modeling. This results is related to the size of the microneedle arrays used in this experiment, which depth approximately 0.1mm-0.15mm, damage can be recovered in a relatively short time. Henry reported [12] that the skin damage caused by 0.77mm microneedle arrays closed after 18 hours, while those caused by 0.37mm microneedle arrays closed after 12 hours, our research results were similar to these.

5. Conclusion

The FN-based complex In Vitro test results confirmed its ability at different concentration:enhance keratinocyte proliferation (+18.28%,10%), Accelerate cell migration (+56.54–60.64%,5-10%); Upregulate barrier-related genes (ZO-1: +18%,10%; IVL: +45%,10); Suppress UVB-induced IL-6 secretion (-48.3%, 10%)

The FN-based complex In vivo test results confirmed that Immediate anti-inflammatory effects (30-min a* value reduction, *p<0.01 vs placebo); sustained barrier restoration (D7 TEWL improvement, *p<0.05), across both microneedle arrays and tape-stripping models.

These results demonstrates multifunctional therapeutic potential for sensitive and damaged skin (SS/DS) management.

References

- [1] He L, Zheng J, Ma HQ, et al. Chinese consensus on diagnosis and treatment of sensitive skin. CHIN J DER M VENER EOL.1(2017):1-4.
- [2] Yang L, Lyu L, Wu W, et al. Genome-wide identification of long non-coding RNA and mRNA profiling using RNA sequencing in subjects with sensitive skin. Oncotarget 8 (2017):114894-114910.
- [3] Effendy I, Loeffler H, Maibach HI, et al. Baseline transepidermal water loss in patients with acute and healed irritant contact dermatitis. Contact Dermatitis. 33(2010): 371–374.

- [4]Stander S, Schneider SW, Weishaupt C, et al. Putative neuronal mechanisms of sensitive skin. *Exp Dermatol.* 18(2010): 417–23.
- [5]Farage MA, Maibach HI. Sensitive skin: closing in on a physiological cause. *Contact Dermatitis* 62(2010): 137–149.
- [6]Roumen Pankov.Kenneth M.Yamada.Fibronectin at a glance *Journal of Cell Science.* 115(2002): 3861-3863.
- [7]Caleb J. Dalton, Christopher A. Lemmon. Fibronectin: Molecular Structure, Fibrillar Structure and Mechanochemical Signaling. *cells.* 10(2021): 1-20.
- [8]Jennifer Patten, Karin Wang. Fibronectin in development and wound healing. *Advanced Drug Delivery Reviews.* 170(2021): 353–368.
- [9]Abir Chakraborty , Natasha Marie-Eraine Boel,et al. HSP90 Interacts with the Fibronectin N-terminal Domains and Increases Matrix Formation, *cells.* 9(2020): 272.
- [10]Garif Yalak, Jau-Ye Shiuld, Ingmar Schoen,et al. Phosphorylated fibronectin enhances cell attachment and upregulates mechanical cell functions. *PLoS ONE* 14(2019): 1-20.
- [11]Renato V. Iozzo1, Liliana SchaeferProteogly can form and function: A comprehensive nomenclature of proteoglycans. *Matrix biology.* (2015):12-54.
- [12]Haripriya K, Chandra SK, and Ajay KB. Characterization of Microchannels Created by Metal Microneedles: Formation and Closure. *The AAPS Journal.* 3(2011): 473-481.